 CMES, vol.52, no.1, pp.83-103, 2009

Computation of Acoustic Far Field Scattering Cross Section from Plain and Intersecting Thin Bodies

P.R. Venkatesh[1], B. Chandrasekhar[2] and M.M.Benal[3]

Abstract: In this work, node based basis functions are used to solve the acoustic scattering from plain thin bodies like plates, discs; and intersecting thin bodies like fins on a cylinder. Node based basis functions are defined on the vertices of triangles generated by triangular patch modeling, and these functions are used to define the unknown source distribution. Also the same functions are used as testing functions in the method of moment's solution. Three kinds of nodes were treated for defining the basis functions, namely, boundary node, non-boundary node and non boundary intersecting node. Also, three kinds of bodies were considered for the acoustic scattering, namely closed bodies, open bodies and intersecting bodies. A common numerical solution procedure is developed for the three kinds of bodies using the node based basis functions. The numerical solutions developed are validated with closed form solutions wherever possible. Also the numerical solutions were used to predict the far fields of complex bodies.

Keywords: Acoustic scattering, Method of moments, Node based basis functions, Boundary integral equations, Acoustic resonance problem, Non-uniqueness, thin bodies, surfaces

1 Introduction

The acoustic scattering from thin objects like plates and discs is attracting considerable attention from researchers since complexities involved in modeling the geometry and developing efficient numerical schemes is challenging. Thin bodies may be defined as those bodies which have its thickness very small compared to its other dimensions. This poses a challenge to create a quality mesh on the surface of the thin bodies as the thickness becomes a deciding factor in the total number of nodes or vertices created. For modeling purposes, as the thickness of the body

[1] Dept of Mechanical Engi neering, RV College of Engineering, Bangalore, India.
[2] Dept of Mechanical Engineering, SRS Institute of Technology, Bangalore, India.
[3] Dept of Mechanical Engineering, Sambhram Institute of Technology, Bangalore, India.

becomes smaller, the number of nodes or vertices generated on the body becomes larger, which puts strain on the computational capacity of the hardware one uses for solving the problem accurately. Hence, more versatile numerical methods are required to treat such problems which have less computational complexity.

Acoustic radiation and scattering problems are popularly solved using boundary element method [Yang (2004), Qian, Han, Ufimtsev & Atluri (2004), Yan, Cui & Hung (2005)] as only the surface of the object needs to be meshed. Other applications of BEM can be found in ref [Tan, Shiah & Lin (2009), Karlis, Tsinopoulos, Polyzos & Beskos (2008), Soares&Vinagre (2008), Mantia & Dabnichki (2008)and Wang & Yao (2008)]. Though BEM is very popular, it has got two major drawbacks. The first one is the final moment matrices being dense and the second one is the presence of singular, strongly singular and hyper singular kernels [De Klerk (2005)] in the boundary integral equations. To overcome the problem of dense matrices there has been a great deal of research work going on using different approaches [He, Lim & Lim (2008), Liu & Nishimura (2006), Phillips & White (1997)]. The treatment of strongly singular and hyper singular kernels has been given a great importance by the researchers to implement it numerically. Notable among them are: calculation techniques of hyper singular integrals [Yan, Hung & Zheng (2003) and Yan, Cui & Hung (2005)], derivation of non-hypersingular boundary integral equations [Qian, Han, Ufimtsev & Atluri (2004), and Qian, Han & Atluri (2004)], derivation of weekly singular and regular integrals [Han & Atluri (2007) and Sanz, Solis & Dominguez (2007)] and usage simple vector calculus operators to circumvent the hyper singularity [Chandrasekhar & Rao (2008), and Chandrasekhar (2008)] in integral equations.

In real world applications, all objects are to be treated as closed. But there are objects which are very thin and can be approximated with a surface. They are called in this work as open bodies since the volume occupied by those thin bodies is very less and can be neglected. There is also another kind of objects which are nothing but intersecting surfaces. An example of this kind object can be a space craft having wings whose thickness is so negligible compared its other dimensions, hence it can be treated, for computational purposes, as a surface intersecting with the main body. If a thin body is treated as a closed body, having definite volume, such bodies are subjected to breakdown of the solutions at their characteristic frequencies [Chen & Chen (2006), Chen, Chen & Chen (2006)]. Where as in case of open bodies and interesting bodies, when treated as surfaces or intersection of surfaces, are not prone to this problem.

Three popularly known methods to resolve the non-uniqueness problem in the exterior acoustic problems of closed bodies are

1. Combined Helmholtz Integral Equation Formulation (CHIEF) [Schenck (1968)],
2. Burton and Miller's (BM) approach [Burton & Miller (1971)] and
3. Method of Moments based Combined Layer Formulation (MoMCLF) [Chandrasekhar & Rao (2004)].

The advantages and limitations of these three methods are discussed in detail in ref [Chandrasekhar & Rao (2008)]. It is possible to extend the MoMCLF to develop a common numerical solution procedure to treat open and intersecting bodies along with the usage of node based basis functions. Open and intersecting bodies were treated in ref [Chandrasekhar & Rao (2005)]. The method of moments /BEM solution that was proposed was based on defining the basis functions on the edges of the triangular patch modeling of the surface of the scattering body. As the method of moments solution results in a full matrix, the size of the resulting impedance matrix, based on defining the basis functions on the edges, is large. Hence it puts a limitation on the hardware as explained in previous paragraphs.

Chandrasekhar has developed a numerical scheme which defines the basis functions on the nodes for solving combined layer formulation (CLF) of closed bodies [Chandrasekhar (2008)]. Compared to defining the basis functions on the edges, it is some what difficult to define the basis functions on the nodes. In other words, procedure to define the basis functions on the nodes is more complex than defining it on the edges. In this work, more complex procedures are developed for defining the basis functions for the nodes located on the open edges and intersection edges of the surfaces. But it is worth using the node based basis functions as it saves enormous amount of computational power due to fewer unknowns. For a closed body, the relationship between the number of nodes N_n, edges N_e and patches N_f in the triangular patch modeling is given by $N_n - N_e + N_f = 2$ and $N_f = 2N_e/3$ [Oneill]; this results into $N_n = 2 + N_e/3$. Thus order of the resulting matrix, defining the basis functions on the nodes, is almost one third to that of defining the basis functions on edges. As the storage matrix is smaller, time required for the solution of simultaneous linear system of equations is smaller and hence, much larger problems can be solved without increasing the solution time compared to the existing solutions based on method of moments with face based basis functions [Raju, Rao & Sun (1991), Rao and Sridhara (1991), Rao, Raju & Sun (1992), Rao & Raju, (1989)] and with edge based basis functions [Chandrasekhar & Rao (2004)]. All the research work discussed above, either use complex numerical procedures to solve hyper singular integral equations, or give special treatment for bodies with sharp edges/corners; and no common algorithms have been developed to approximate the thin bodies as open bodies except ref [Chandrasekhar & Rao (2005)]. It is a step forward, in this research work, to develop an algorithm with a simple and common

(to closed, open and intersecting bodies) numerical procedure to compute far fields by treating the thin bodies as open bodies which finally results in smaller size of moment matrix.

In this work, three kinds of nodes were treated for defining the basis functions, namely, boundary node, non-boundary node and non boundary intersecting node. Also, three kinds of bodies were considered for the acoustic scattering, namely closed bodies, open bodies and intersecting bodies. A common numerical solution procedure is developed for the three kinds of bodies using the node based basis functions. Since the closed bodies do have internal resonance problem, combined layer formulation is used for the solution. Open and intersecting bodies do not have the problem of internal resonance and hence they can be solved using double layer formulation to reduce the computational time.

2 Organization of the paper

In this paper, next section briefly describes the method of moment's solution procedure [Harrington (1968), Sun & Rao (1992)]. Mathematical formulation is laid in section 4 for CLF. In section 5, the basis functions are developed for the nodes located on the open edges, intersecting edges and interior edges of the surfaces. In section 6, we derive matrix equations for CLF. Numerical results, based on the development of new basis functions are given in section 7. Lastly we present some important conclusions drawn from the present work.

3 Outline of Method of Moments

Consider the deterministic equation

$$Lf = g \tag{1}$$

where L is a linear operator, g is a known function and f is an unknown function to be determined. Let f be represented by a set of known functions $f_j,\ j = 1,2,...,N$ termed as basis functions in the domain of L as a linear combination, given by

$$f = \sum_{n=1}^{N} \beta_j f_j \tag{2}$$

where β_j are scalar coefficients to be determined. Substituting Eq. 2 into Eq. 1, and using the linearity of L, we have

$$\sum_{n=1}^{N} \beta_j L f_j = g \tag{3}$$

where the equality is usually approximate. Let $(w_1, w_2, w_3, ...)$define a set of testing functions in the range of L. Now, taking the inner product of Eq. 3 with each w_i and using the linearity of inner product defined as $\langle f, g\rangle = \int_s f \bullet g \, ds$, we obtain a set of linear equations, given by

$$\sum_{n=1}^{N} \beta_j \left\langle w_i, L f_j \right\rangle = \langle w_i, g\rangle \quad i = 1, 2, ..., N. \tag{4}$$

The set of equations in Eq. 4 may be written in the matrix form as

$$ZX = Y \tag{5}$$

which can be solved for X using any standard linear equation solution methodologies. The simplicity, accuracy and efficiency of the method of moments lies in choosing proper set of basis/testing functions and applying to the problem at hand. In this work, we propose a special set of basis functions and a novel testing scheme to obtain accurate results using SLF, DLF and CLF.

4 Mathematical Formulation

Consider an acoustic wave, with a pressure and velocity $\left(p^i, u^i\right)$, incident on a three-dimensional arbitrarily shaped rigid body placed in a source free homogeneous medium of density ρ and speed of sound c through the medium. When an incident wave interacts with the body, the acoustic wave gets scattered with a pressure and velocity (p^s, u^s). Here, we note that, incident fields are defined in the absence of the scattering body. Φ is the scalar velocity potential satisfying the Helmholtz differential equation $\nabla^2\Phi + k^2\Phi = 0$ for the time harmonic waves present in the region exterior to the surface S of the body. One more condition on velocity potential is that it should satisfy the appropriate boundary conditions on the surface S of the body along with the Sommerfeld radiation condition. The pressure and velocity fields of acoustic wave is related to the scalar velocity potential Φ as $u = -\nabla\Phi$ and $p = j\omega\rho\Phi$. In this paper, integral equation formulations are based on potential theory and free space Green's function. The scattered velocity potential may be defined using three different formulations based on monopole and/or dipole distribution. Formulations based on monopole distribution and dipole distribution are called as single layer formulation (SLF), double layer formulations (DLF), respectively. Third formulation, namely Combined layer formulation (CLF) is a linear combination of SLF and DLF.

Using the potential theory and the free space Green' s function, the scattered velocity potential Φ^s may be defined as

$$\Phi^s = \int_s \sigma\left(r'\right) G\left(r, r'\right) \, ds' \tag{6}$$

for SLF,

$$\Phi^s = \int_s \sigma\left(r'\right) \frac{\partial G\left(r,r'\right)}{\partial n'} ds' \tag{7}$$

for DLF, and

$$\Phi^s = \int_s \sigma\left(r'\right) G\left(r,r'\right) ds' + \alpha \int_s \sigma\left(r'\right) \frac{\partial G\left(r,r'\right)}{\partial n'} ds' \tag{8}$$

for CLF.

In the above three equations, σ is the source density function independent of r over the surface of the body, r and r' are the position vectors of observation and source points, respectively, with respect to a global co-ordinate system O, and $\partial G/\partial n'$ is the normal derivative of Green's function at source point . Coefficient α is a complex coupling parameter, to be chosen based on the guidelines given by Burton and Miller [Burton and Miller (1971)].

$$k \text{ real or imaginary } \Rightarrow Im(\alpha) \neq 0 \tag{9}$$

$$k \text{ complex } \Rightarrow Im(\alpha) = 0 \tag{10}$$

where k is the wave number in the medium.

$G\left(r,r'\right)$ is the free space Green's function, given by,

$$G\left(r,r'\right) = \frac{e^{-jk|r-r'|}}{4\pi\left|r-r'\right|} \tag{11}$$

$G\left(r,r'\right)$ is the solution of the Helmholtz equation with a point source inhomogeneity

$$\left(\nabla^2 + k^2\right) G(r,r') = -\delta\left(r-r'\right) \tag{12}$$

and can be interpreted as the solution at the observation point r due to the presence of acoustic source of unit strength located at the source point r'.

For a rigid body, the normal derivative of total velocity potential, which is the sum of incident and scattered velocity potential, with respect to the observation point on the surface of the body vanishes. That is

$$\frac{\partial\left(\Phi^i + \Phi^s\right)}{\partial n} = 0 \tag{13}$$

$$\frac{\partial \Phi^s}{\partial n} = -\frac{\partial \Phi^i}{\partial n}. \tag{14}$$

Substituting Eqs. 6, 7 and 8. into Eq. 14,

$$\frac{\partial}{\partial n}\int_s \sigma\left(r'\right) G\left(r,r'\right)\, ds' \;=\; -\frac{\partial \Phi^i}{\partial n} \tag{15}$$

for SLF,

$$\frac{\partial}{\partial n}\int_s \sigma\left(r'\right) \frac{\partial G\left(r,r'\right)}{\partial n'}\, ds' \;=\; -\frac{\partial \Phi^i}{\partial n} \tag{16}$$

for DLF, and

$$\frac{\partial}{\partial n}\int_s \sigma\left(r'\right) G\left(r,r'\right)\, ds' + \alpha\,\frac{\partial}{\partial n}\int_s \sigma\left(r'\right) \frac{\partial G\left(r,r'\right)}{\partial n'}\, ds' = \; -\frac{\partial \Phi^i}{\partial n} \tag{17}$$

for CLF.

In the above equations, Φ^i is the scalar velocity potential of the incident wave.

Eq. 15, the SLF can also be re-written as

$$\frac{\sigma\left(r'\right)}{2} - \int_s \sigma\left(r'\right) \frac{\partial G\left(r,r'\right)}{\partial n} ds' = \; \frac{\partial \Phi^i}{\partial n}. \tag{18}$$

The second term in the above equation is the integration over the surface excluding the principal value term i.e. $r = r'$. We note that, this integral is a well behaved integral, although rapidly varying, which can be evaluated using standard integration algorithms.

Following the procedures developed in [Maue (1949) and Mitzner (1966)], Eq. 16, the DLF, may be written as

$$\int_s n \bullet n' k^2 \sigma(r') G(r,r') ds' + \int_s \left(n' X\, \nabla' \sigma\right) \bullet \left(n X\, \nabla G\right)\, ds' = \frac{\partial \Phi^i}{\partial n} \tag{19}$$

where n and n' are the unit normal vectors at r and r', respectively.

From Eq. 18 and Eq. 19, the CLF can be written as

$$\frac{\sigma\left(r'\right)}{2} - \int_s \sigma\left(r'\right) \frac{\partial G\left(r,r'\right)}{\partial n} ds' + \alpha \int_s n \bullet n' k^2 \sigma(r') G(r,r') ds' + \alpha \int_s \left(n' X\, \nabla' \sigma\right) \bullet \left(n X\, \nabla G\right)\, ds' = \; \frac{\partial \Phi^i}{\partial n}. \tag{20}$$

In the following sections, a novel numerical technique is developed using node based basis functions for CLF. For this, first the basis functions are defined for the nodes located on open edges, interior edges and intersecting edges of a surface. Next, these basis functions are used for defining a source density function in the method of moments solution procedure.

5 Definition of Basis Functions

Fig.1 shows the triangular patch modeling of the surfaces of a arbitrarily shaped three dimensional bodies of three varieties. One is a closed body in which there are no open boundaries, the second one is an open body which is nothing but a surface, and the third one is an intersecting body in which there are intersecting surfaces. The three bodies shown in Fig. 1 are having a shape of a regular cone or it resembles a cone. The triangular patch modeling is an approximation of the surfaces. The accuracy of approximation can be increased by modeling the surface with large number of triangular patches of smaller size. The three geometric entities that are present in the triangular patch modeling are triangular patches, edges and nodes. Let N_f, N_e and $N_n$represent the number of triangular patches, number of edges and number of nodes, respectively, on the surface of triangulated body. For a closed body, every edge is common to two adjacent triangular patches, and every node is common to at least three triangular patches as well as at least three edges. Where as in case of an open body, there are edges which have only one adjacent triangular patch, and they are called as boundary edges and the corresponding nodes of that edge are called as boundary nodes in this paper. Similarly, in case of intersecting bodies, there are edges which has more than two triangular patches; and these edges are called as interesting edges and the corresponding nodes are called as intersecting nodes.

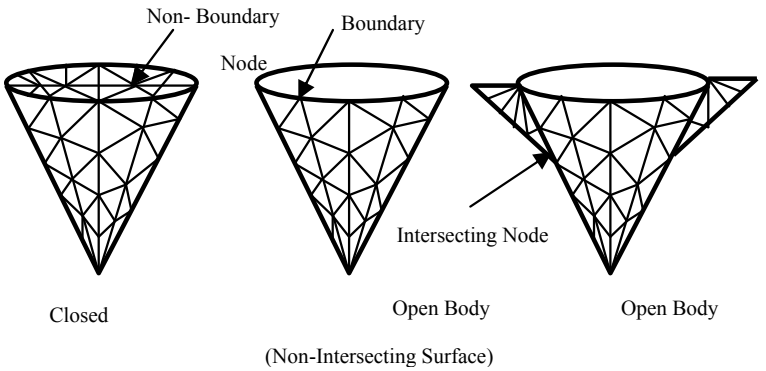

Figure 1: Triangular patch modeling of an Cone shaped three-dimensional bodies.

Next, we develop basis functions for these three kinds of nodes and they will be used in the method of moments solution procedure to calculate the far field cross sections of different bodies.

A. Non Boundary Node:

Consider a node n about which the basis function is defined. For illustration purposes, consider one such node as shown in Fig. 2, where there are five triangular patches attached to it. Let $T_1, T_2, ..., T_5$ are the triangular patches and $e_1, e_2, ..., e_5$ are the edges surrounding the node. The shaded region, shown in the Fig. 2. as S_n, is formed by joining the mid points of the edges, that are connected to the node n, to the centroids of adjacent triangular patches thus forming a closed boundary around the node.

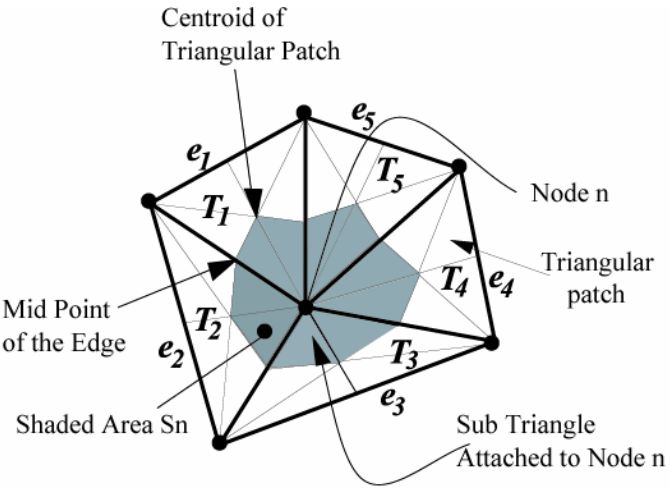

Figure 2: Node based basis function and geometric parameters associated with the node.

Since the method of moments solution calls for the definition of expansion/basis as well as testing/weighting functions, expansion/basis functions are defined on the source node n and the testing/weighting functions are defined on the field node m. Let there are p number of triangular patches attached to field node m and q number of triangular patches attached the source node n. By joining the node on which the basis function or weighting function is defined, to the centroid of the attached triangular patches, the shaded area on each triangular patch is divided into two sub triangles, resulting u number of sub triangles around field node m and v number of sub triangles around the source node n. In this paper, index x is used to represent the sub triangle attached to the field node and index y is used to represent the sub triangle attached to the source node.

The node based basis function is defined over the shaded area as follows.

$$f_n\left(r'\right) = \begin{cases} 1 & r' \in S_n \\ 0 & Otherwise. \end{cases} \tag{21}$$

The source density function σ over the surface of the scattering object is approximated by

$$\sigma\left(r'\right) = \sum_{n=1}^{N_n} \beta_n f_n \tag{22}$$

where β_n represent the unknown coefficients to be determined and the equality sign is usually approximate. The basis functions defined over the node has all advantages as edge based basis functions [see B. Chandrasekhar & Rao (2004)].

In the numerical solution of CLF, Galarkin's approach is used by defining the testing function in the same manner as it is defined for the basis function.

$$w_m = \begin{cases} 1 & r \in S_m \\ 0 & Otherwise. \end{cases} \tag{23}$$

B. Boundary Node

A boundary node is a one which is located on the boundary edges of an open body. The position of boundary node is depicted in Fig. 1. Since the basis function do not surround the node as in the case of non-boundary node, it is difficult to treat these nodes due to the way the numerical solutions are described in the later sections. For this purpose one can choose the following option. As in case of electromagnetic scattering from open bodies, one can assume that there are no sources located on the edges; hence the boundary nodes are discounted from the number of unknowns. In order to minimize the error arising due to this assumption, one can increase the density of triangular patches at the boundary. Hence

$$f_n\left(r'\right) = \begin{cases} 1 & r' \in S_n \; and \; r' \notin \Gamma \\ 0 & Otherwise. \end{cases} \tag{24}$$

where Γ is the boundary of a open surface.

C. Intersecting Non-Boundary Node

A node can be defined as an intersecting node if any of the edges sharing it have more than two triangular patches attached to it. For example in Fig. 3a, an intersecting node is shown and the procedure to define basis functions is laid down

as follows. Group the triangular patches attached to the intersecting node into different sets. Care should be taken in a such a way that each set when combined with any other set, it should be possible to completely define node based basis function as described in above sections. For example, for the intersecting node shown in Fig 3a, three sets can be formed. They are (P_a, P_b, P_c), (P_d, P_e, P_f) and (P_g, P_h). A node based basis function can be defined by adding any two of the three sets. The possible combinations are $(P_a, P_b, P_c, P_d, P_e, P_f)$, $(P_a, P_b, P_c, P_g, P_h)$ and $(P_d, P_e, P_f, P_g, P_h)$. Figs. 3b and 3c shows the node based basis function for the combined sets $(P_a, P_b, P_c, P_d, P_e, P_f)$ and $(P_a, P_b, P_c, P_g, P_h)$. If there are N sets attached to the intersecting node, then the number of basis functions required for defining the source density function is $N-1$.

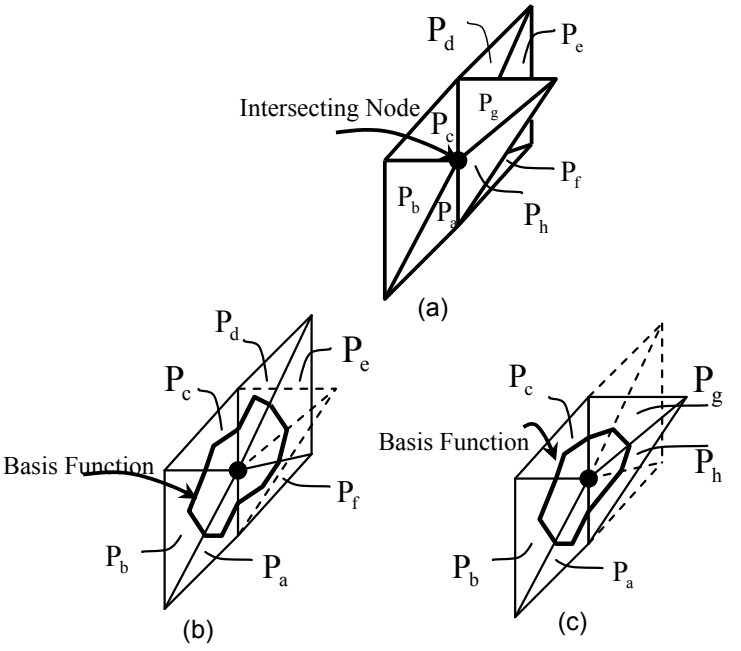

Figure 3: Basis functions on a node located on the intersecting edges.

6 Numerical Solution Procedure

In this section the matrix equations are presented for the combined layer formulation using node based basis functions. The detailed derivation of the matrix equation for combined layer formulation using node based basis functions can be found in ref [Chandrasekhar (2008)].

Testing Eq. 20 with the functions defined in Eq. 23

$$\left\langle w_m, \frac{\sigma(r')}{2} \right\rangle - \left\langle w_m, \int_s \sigma\left(r'\right) \frac{\partial G(r,r')}{\partial n} ds' \right\rangle + \alpha \left\langle w_m, \int_s n \bullet n' k^2 \sigma(r') G(r,r') ds' \right\rangle + \alpha \left\langle w_m, \int_s \left(n' x \nabla' \sigma\right) \bullet (nX \nabla G)\, ds' \right\rangle = \left\langle w_m, \frac{\partial \Phi^i}{\partial n} \right\rangle. \quad (25)$$

This can be expressed in matrix form as

$$Z_{clf}^{mn} X = Y^m \quad (26)$$

where

$$Z_{clf}^{mn} = Z_{slf}^{mn} + \alpha Z_{dlf}^{mn} \quad (27)$$

Z_{slf} and Z_{dlf} are the impedance matrices of the single layer and double layer formulations of size $N_n X N_n$, X and Y are column vector of size N_n.

$$Z_{slf}^{mn} = \begin{cases} \frac{1}{2} \sum_{x=1}^{u} A_m^x & form = n and x = y \\ -\sum_{x=1}^{u} \sum_{y=1}^{v} A_m^x \int_s \frac{\partial G\left(r_m^{cx}, r_n^{cy}\right)}{\partial n_m^x} ds' & otherwise \end{cases} \quad (28)$$

where r_m^{cx} is the position vector to the centroid of the x^{th} sub-triangle attached to field node, r_n^{cy} is the position vector to the centroid of the y^{th} sub-triangle attached to source node and $\partial G / \partial n_m^x$ is the normal derivative of Green's function at the centroid of the x^{th} sub-triangle attached to field node.

$$Z_{dlf}^{mn} = \sum_{x=1}^{u} \sum_{y=1}^{v} k^2 A_m^x n_m^x \bullet n_n^y \int_s G(r_m^{cx}, r_n^{cy}) ds' + \frac{l_m}{2} \bullet \frac{l_n}{2A_{fn}} \left(\sum_{x=1}^{p} \sum_{y=1}^{q} \int_{sf} G\left(r_m^{cfp}, r_n^{cfq}\right) ds' \right). \quad (29)$$

and

$$Y^m = \sum_{x=1}^{u} A_m^x \frac{\partial \Phi^i\left(r_m^{cx}\right)}{\partial n_m^x} \quad (30)$$

where A_m^x is the area of the sub triangle attached to the field node, A_{fn} is the area of the triangular patch attached to the source node, r_m^{cx} is the position vector to the

centroid of the x^{th} sub triangle attached to field node, r_n^{cy} is the position vector to the centroid of the y^{th} sub triangle attached to source node, r_m^{cfp} is the position vector to the centroid of the p^{th} triangular patch attached to field node, and r_n^{cfq} is the position vector to the centroid of the q^{th} triangular patch attached to source node. n_m^x and n_n^y represent the unit normal vectors of the sub triangle connected to the m^{th} node and n^{th} node respectively. l_m and l_n the vectors of the edges of corresponding nodes as shown in Fig 4.

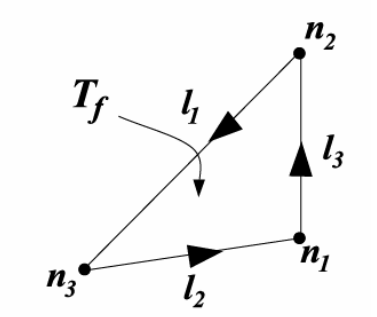

Figure 4: Triangular patch T_f and associated edges and nodes.

For a plane wave incidence, we set

$$\Phi^i = e^{jk\hat{k}\bullet r} \tag{31}$$

where the propagation vector $\hat{k}$ is given by,

$$\hat{k} = \sin\theta_0 \cos\phi_0 \, a_x + \sin\theta_0 \sin\phi_0 \, a_y + \cos\theta_0 \, a_z \tag{32}$$

(θ_0, ϕ_0) define the angles of arrival of the plane wave in the conventional spherical co-ordinate system and a_x, a_y and a_z are the unit vectors along the x, y and z axes, respectively.

The normal derivative of the incident field may be written as

$$\frac{\partial \Phi^i}{\partial n} = n \bullet \nabla \Phi^i = jk n \bullet \hat{k} e^{jk\hat{k}\bullet r}. \tag{33}$$

Once the elements of the impedance matrix Z and the forcing vector Y are determined, one may solve the linear system of equations, Eq. 26 for the unknown vector X using any standard matrix inversion techniques.

7 Numerical Results

In this section, numerical results for the numerical solutions based on using any or combination of three different basis functions are presented depending up on the geometry of the scattering body. Also, three kinds of bodies are considered in the numerical results, namely, closed bodies, open bodies and intersecting bodies. The closed bodies were solved with CLF where as the open and intersecting bodies were solved using DLF since there are no resonance frequencies associated with open and intersecting bodies. However, one can use CLF numerical solution procedure for open and intersecting bodies also. The geometries considered are a disc, a rectangular plate, a rectangular plate intersecting with a square plate, and a body with an aircraft like shape. To begin with the node based CLF numerical solution is validated for a case of a circular disc since a closed form solution [Bowman, Senior & Uslenghi (1969)] is available for a circular disc. Along with the CLF solution, a node based open body DLF solution is validated against the CLF solution and closed form solution. Later on, the DLF solutions for open and intersecting bodies were compared with the CLF solutions for those cases which do not have closed form solutions.

Fig. 5 shows the geometries of the three cases validated in this work. Fig. 5a shows the geometry of a disc of radius 1m. The normal of the disc is aligned with the Z-axis and the acoustic plane wave is traveling in –Z direction and incident on the disc. The disc is modeled as a open body (surface) as well as a closed body. The open body is approximated by 121 nodes and 340 edges. Similarly, closed body is modeled as 0.01m thick with 242 nodes and 720 edges. The number of nodes and edges in case of a closed body is more since the there are two circular surfaces and a cylindrical surface compared to one circular surface as in case of a disc modeled as an open body.

Fig. 6 shows Scattering cross section versus polar angle for an acoustically rigid disc of radius 1m, subjected to an axially incident plane wave of $k = 1\, rad/m$traveling in –Z direction. The closed body is solved using CLF($\alpha = 0.1\, j$); where as the open body is solved using DLF. Both the solutions are compared with the closed form solution. The scattering cross section for the numerical solution is defined by

$$\begin{aligned} S &= 4\pi \left| \frac{\Phi^s}{\Phi^i} \right|^2 \\ &\approx \frac{1}{4\pi} \left| \sum_{n=1}^{N_n} \beta_n \left[\sum_{y=1}^{v} A_n^y n_n^y \bullet r_n^y e^{jkn_n^y \bullet r_n^y} \right] \cdot \right|^2 \end{aligned} \tag{34}$$

The solutions compare very well with the closed form solution. The accuracy of the solutions can be further improved by increasing the number of triangular patches

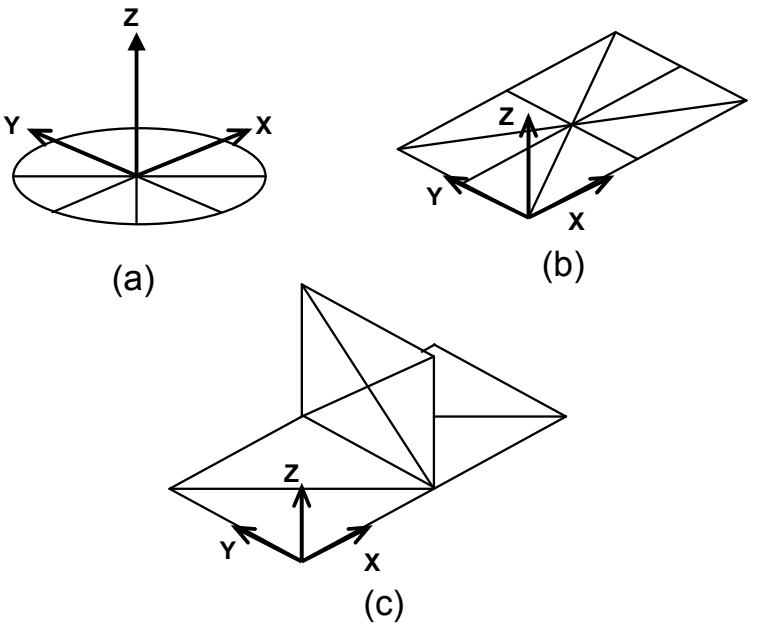

Figure 5: Geometries of thin and intersecting bodies

for the case of open body; and reducing the thickness of the disc and increasing the number of triangular patches for the case of closed body. However it is not the scope of the present work to optimize the number triangular patches for a given accuracy of solution.

Fig. 5b shows a rectangular thin plate of dimensions 2m$\times$1m. The plate has been modeled as closed body with thicknesses 0.01m and 0.001 m for demonstrating the convergence of solution towards open body solution. The closed body model of the rectangular plate has been modeled with 462 nodes and 1380 edges; where as the open body model is modeled with 231 nodes and 630 edges.

It is evident from Fig. 7 that open body solution is very close to the solution of the closed body having lesser thickness. As the thickness of the closed body model of the plate is reduced from 0.01m to 0.001m, its solution converges towards the open body model. The open body model of both disc and plate uses boundary node basis function and non-boundary node basis functions in the numerical solution.

Fig. 5c shows the geometry of a rectangular plate of dimensions 2m x 1m with negligible thickness intersecting with a square plate of size 1m x 1m. This geometry may be again modeled as a closed body with thicknesses of 0.01m and 0.001m, and as a open body. The closed body is modeled with 704 nodes and 2106 edges; where

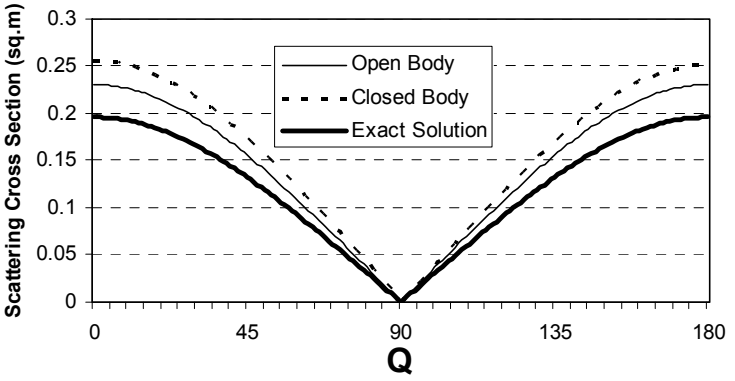

Figure 6: Scattering cross section versus polar angle for an acoustically rigid disc of radius 1m, subjected to an axially incident plane wave of $k = 1\,rad/m$.

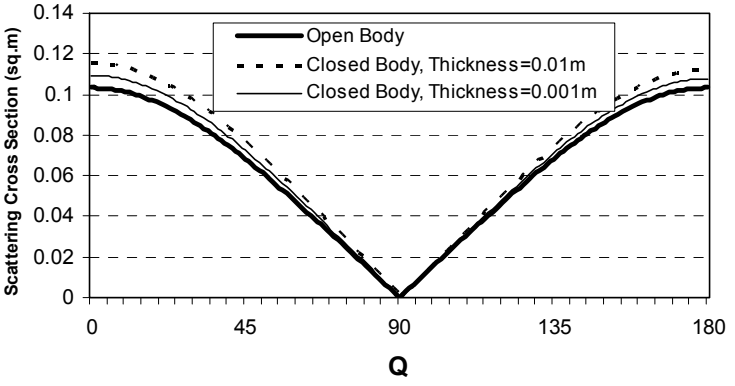

Figure 7: Scattering cross section versus polar angle for an acoustically rigid rectangular thin plate of size 2m x 1m, subjected to an axially incident plane wave of $k = 1\,rad/m$.

as the open body model is approximated with 341 nodes and 940 edges.

It is evident from Fig. 8 that as the thickness of the plates is reduced from 0.01m to 0.001m, the far field scattering cross section converges towards the open body solution. In other words, the open body solution compares very well with the closed body solution as thickness of the plates is reduced. This is a case where all kinds of basis functions developed in this work, namely, boundary node basis functions, non-boundary node basis functions and intersecting node basis functions are used in the numerical solution.

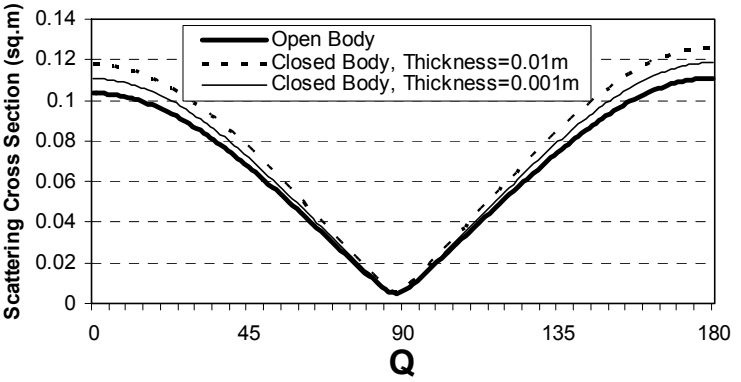

Figure 8: Scattering cross section versus polar angle for an acoustically rigid intersecting thin plates, subjected to an axially incident plane wave of $k = 1\,rad/m$

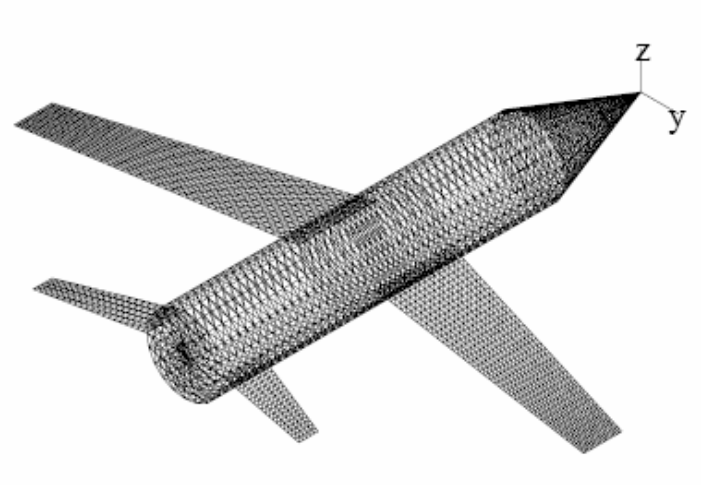

Figure 9: Triangulated model of an aircraft like body.

As a final case, the numerical solution developed in this work is used to solve for a case of an aircraft like body shown in Fig. 9. The wings of the body are modeled as open bodies and the main body is modeled as a closed body. This is an example of open bodies intersecting with a closed body. The overall size of the cylindrical body is 2m in diameter and 12.5m in length. The size of the main wings is 2m x 6.5m and that of small wings in the rear is 0.5m x 2.5 m. The body is approximated by triangular patch modeling with 3222 nodes and 9420 edges.

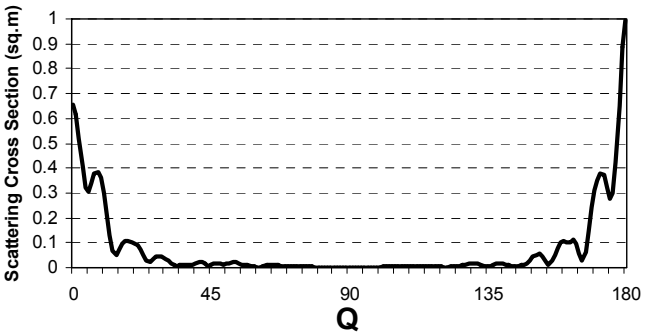

Figure 10: Scattering cross section (normalized) versus polar angle for an acoustically rigid aircraft like body, subjected to an axially incident plane wave of $k = 1\,rad/m$

Fig. 10 shows the normalized scattering cross section versus polar angle for an acoustically rigid aircraft like body, subjected to an axially incident plane wave of $k = 1\,rad/m$ traveling in –Z direction. The numerical solution uses again all the three kinds of basis functions defined above.

8 Conclusions

In this work, node based basis functions are used to solve the acoustic scattering from plain thin bodies like plates, discs; and intersecting thin bodies like wings on a cylinder. Node based basis functions are defined on the vertices of triangles generated by triangular patch modeling, and these functions are used to define the unknown source distribution. Also the same functions are used as testing functions in the method of moment's solution. Three kinds of nodes were treated for defining the basis functions, namely, boundary node, non-boundary node and non boundary intersecting node. Also, three kinds of bodies were considered for the acoustic scattering, namely closed bodies, open bodies and intersecting bodies. A common numerical solution procedure is developed for the three kinds of bodies using the node based basis functions. The numerical solutions developed are validated with closed form solutions wherever possible. To validate the numerical solutions, a case of acoustic scattering from disc is solved since the disc has a closed form solution. The numerical solutions compare very well with the closed form solution. Also, the closed body solutions are validated with the closed form solutions. For the cases of a rectangular plate and intersecting plates, the open body solutions are compared with the closed body solutions based on CLF. For lesser and lesser thickness of the plates, the open body solutions converge towards closed body solutions. All three

kinds of basis functions developed in this work are validated by using them in the solutions for a case of intersecting plates. Also the numerical solutions were used to predict the far fields of complex bodies like aircraft like bodies. This work can be further improved by using adaptive basis functions.

References

Bowman, J.J.; Senior, T.B.A.; Uslenghi, P.L.E. (1969): Electromagnetic and Acoustic Scattering by Simple Shapes North-holland, Amsterdam.

Burton, A.J.; Miller, G.F. (1971): The application of integral equation methods to the numerical solution of some exterior boundary value problems. *Proceedings of Royal Society, London* vol A323, pp. 601-618 .

Chandrasekhar, B.; Rao, S.M. (2004): Elimination of internal resonance problem associated with acoustic scattering by three-dimensional rigid body, *Journal of Acoustical Society of America,* vol 115, pp. 2731-2737.

Chandrasekhar, B.; Rao, S.M. (2005): Acoustic Scattering from Complex Shaped Three Dimensional Structures, *CMES: Computer Modeling in Engineering & Sciences*, vol. 8, No. 2, pp. 105-118.

Chandrasekhar, B. (2008): Node Based Method of Moments Solution to Combined Layer Formulation of Acoustic Scattering. *CMES: Computer Modeling in Engineering and Sciences*, Vol. 33, No. 3, pp. 243-268.

Chandrasekhar, B.; Rao, **S.M.** (2008): A New Method to Generate an Almost-Diagonal Matrix in The Boundary Integral Equation Formulation. *Journal of Acoustical Society of America,* Vol. 124, Issue no. 6, pp. 3390-3396.

Chen, I.L.; Chen, K.H.(2006), Using the Method of Fundamental Solutions in Conjunction with the Degenerate Kernel in Cylindrical Acoustic Problems, *J. Chinese Institute of Engineers,* vol 29, No.3, 445-457.

Chen, J.T.; Chen, I.L.; Chen, K.H.(2006) A unified formulation for the spurious and fictitious frequencies in acoustics using the singular value decomposition and Fredholm alternative theorem, *J. Comp. Acoustics,* vol 14, No.2, 157-183.

De Klerk J.H. (2005): Hypersingular integral equations—past, present, future. *Nonlinear Analysis,* 63: 533 –540.

Harrington, R.F. (1968): Field computation by Method of Moments. *MacMillan, New York*.

Han Z.D.; Atluri S.N. (2007):A systematic approach for the development of weaklysingular BIEs, *CMES: Computer Modeling in Engineering & Sciences*, 21(1): 41-52. (9)

He X.F.; Lim K.M.; Lim S.P. (2008): Fast BEM Solvers for 3D Poisson-Type

Equations. *CMES: Computer Modeling in Engineering & Sciences*, 35(1): 21-48.

Karlis G.F.; Tsinopoulos S.V.; Polyzos D.; Beskos D.E. (2008): 2D and 3D boundary element analysis of mode-I cracks in gradient elasticity. *CMES: Computer Modeling in Engineering & Sciences*, 26(3): 189-207.

Liu Y.J.; Nishimura N. (2006): The fast multipole boundary element method for potential problems: A tutorial. *Engineering Analysis with Boundary Elements*, 30(5): 371-381.

Mantia M.L.; Dabnichki P. (2008): Unsteady 3D boundary element method for oscillating wing. *CMES: Computer Modeling in Engineering & Sciences*, 33(2): 131-153.

Maue, A.W. (1949): Zur Formulierung eines allgemeinen Beugungsproblems durch eine Integralgleichung. *Journal of Physics*, vol 126, pp. 601-618.

Mitzner, K.M. (1966): Acoustic scattering from an interface between media of greatly different density. *Journal of Mathematical Physics*. vol 7, pp. 2053-2060.

O'Neill. B. (1966): Elementary Differential *Geometry. Academic, New York.*

Phillips J.R.; White J.K. (1997): A precorrected-FFT method for electrostatic analysis of complicated 3-D structures. *IEEE Transactions on Computer-aided Design of Integrated Circuits and Systems*, 16(10): 1059-1072.

Qian Z.Y.; Han Z.D.; Atluri S.N. (2004): Directly derived non-hypersingular boundary integral equations for acoustic problems, and their solution through Petrov Galerkin schemes. *CMES: Computer Modeling in Engineering & Sciences* 5(6): 541-562.

Qian Z.Y.; Han Z.D.; Ufimtsev P.; Atluri S.N. (2004): Non-hypersingular boundary integral equations for acoustic problems, implemented by the collocation-based boundary element method. *CMES: Computer Modeling in Engineering & Sciences* 6(2): 133-144.

Raju, P.K.; Rao, S. M.; Sun, S.P. (1991): Application of the method of moments to acoustic scattering from multiple infinitely long fluid filled cylinders. *Computers and Structures.* vol 39, pp. 129-134.

Rao, S.M.; Raju, P.K. (1989): Application of Method of moments to acoustic scattering from multiple bodies of arbitrary shape. *Journal of Acoustical Society of America*. vol 86, pp. 1143-1148.

Rao, S.M.; Sridhara, B.S. (1991): Application of the method of moments to acoustic scattering from arbitrary shaped rigid bodies coated with lossless, shearless materials of arbitrary thickness. *Journal of Acoustical Society of America*. vol 90, pp. 1601-1607.

Rao, S. M.; Raju, P.K.; Sun, S.P. (1992): Application of the method of moments

to acoustic scattering from fluid-filled bodies of arbitrary shape. *Communications in Applied Numerical Methods*, vol 8, pp. 117-128.

Soares Jr.D.; Vinagre, M. P. (2008): Numerical computation of electromagnetic fields by the time-domain boundary element Method and the complex variable method. *CMES: Computer Modeling in Engineering & Sciences*, 25(1): 1-8.

Sanz J.A.; Solis M.; Dominguez J. (2007): Hypersingular BEM for piezoelectric solids: formulation and applications for fracture mechanics, *CMES: Computer-Modeling in Engineering & Sciences*, 17(3): 215-229.

Schenck, H.A (1968): Improved integral formulation for acoustic radiation problems. *Journal of Acoustical Society of America.* vol 44, pp. 41-58.

Sun, S.P.; Rao, S. M. (1992): Application of the method of moments to acoustic scattering from multiple infinitely long fluid-filled cylinders using three different formulation. *Computers and Structures*. vol 43, pp. 1147-1153.

Tan C.L.; Shiah Y.C.; Lin C.W. (2009): Stress Analysis of 3D Generally Anisotropic Elastic Solids Using the Boundary Element Method. *CMES: Computer Modeling in Engineering & Sciences*, 41(3): 195-214.

Wang H.T.; Yao Z.H. (2008): A rigid-fiber-based boundary element model for strength simulation of carbon nanotube reinforced composites. *CMES: Computer Modeling in Engineering & Sciences*, 29(1): 1-13.

Yan Z.Y.; Hung K.C.; Zheng H. (2003): Solving the hypersingular boundary integral equation in three-dimensional acoustics using a regularization relationship.

J. Acoust. Soc. Am. 113: 2674-2683.

Yan Z.Y.; Cui F.S.; Hung K.C. (2005): Investigation on the normal derivative equation of Helmholtz integral equation in acoustics. *CMES: Computer Modeling in Engineering & Sciences,* 7(1)**:** 97-106.

Yang S.A. (2004): An integral equation approach to three-dimensional acoustic radiation and scattering problems. *J. Acoust. Soc. Am.* 116 (3): 1372-1380.